Received: Added at production | Revised: Added at production | Accepted: Added at production

DOI: xxx/xxxx

ARTICLE TYPE

Analysis of the accuracy on computing nominal stress in a biaxial test for arteries.

M. Cilla[1,2,3] | A. V. Corral[1] | J.A. Peña[4] | E. Peña*[1,2]

[1]Aragón Institute of Engineering Research (I3A), University of Zaragoza, Spain
[2]CIBER de Bioingeniería, Biomateriales y Nanomedicina, (CIBER-BBN), Spain
[3]Centro Universitario de la Defensa, Academia General Militar. Zaragoza, Spain
[4]Department of Management and Manufacturing Engineering. Faculty of Engineering and Architecture, University of Zaragoza, Spain

Correspondence
*Estefanía Peña, Mechanical Engineering Department. c/ Maria de Luna s/n 50018. Zaragoza. Spain. Tel.: +34 876555233.
Email: fany@unizar.es

Summary

Biaxial tests are commonly used to investigate the mechanical behaviour of anisotropic soft biological tissues such as cardiovascular tissues. However, there is still no clear understanding of the influence that the biaxial test setup conditions may have on the computing material stress of the experimental results. The aim of the present study is to further investigate the accuracy of calculated material stress from measured force during biaxial tests using Finite Element Methods (FEM). The biaxial mechanical response of ascending aorta and pulmonary artery tissue samples was obtained by FEM simulation under two different gripping methods: (i) a system with noodle clamps and (ii) a clamped system with needles which leave the specimen's edges free to expand laterally.

The results show that the clamped method whose joints allow free movement in the lateral direction produces stresses closer to the universally accepted formulation of biaxial material stress in the central region. However, the system with noodle clamps, commonly used to grip the sample, produces an alteration of the measurement stresses. Our simulations show results giving an inaccurate estimation of the stress at the centre of the sample. In some cases the stresses are overestimated, and in others underestimated depending on the anisotropy of the sample. We can conclude that the clamped system with needles which leave the specimen's edges free to expand laterally should be used as an efficient methodology to other commonly used gripping methods for biological tissues with anisotropic materials.

KEYWORDS:
Uniaxial and biaxial testing, Ascending aorta artery, Pulmonary artery, Constitutive modeling, Hyperelastic material

1 | INTRODUCTION

Cardiovascular diseases (CVD) are the number one cause of death globally. More people die annually due to these diseases than from any other cause. An estimated 17.7 million people died from CVDs in 2015, representing 31% of all global deaths [52]. In recent years, computational biomechanics has become an emerging research field that seeks to understand the complex mechanical behaviours of normal and pathological human systems and to come up with new methods of treatment and/or devices. Specifically, biomechanical computational models based on different numerical methods such as Finite Element Methods (FEMs) are now used in risk assessment of CVDs. These complex computational models require, among others, constitutive

equations of the vascular tissue, which reproduce the mechanical response of the cardiovascular system. For this reason, the experimental study of the mechanical properties of biological tissues and, in particular, of vascular tissues, is of crucial importance. In order to obtain the material properties of these tissues, the classical engineering testing techniques have been applied to biological materials [see e.g., 9, 11, 23, and references therein] and a large number of experiments have been conducted over the years on measuring the structural and functional properties of biological tissues. Nevertheless, the particular characteristics of these tissues noticeably complicate the obtaining of valid results and the standardization of these measurements and consequently the interpretation of results is difficult to establish. Several factors such as the test conditions [21, 32], the tissue degeneration [45], the geometry and size of the sample [3, 35, 46], the device for gripping the sample edges [7] or the method to determine the stress [34, 46] may have effects on the measured mechanical properties.

As regards the testing procedures used for the characterization of the vascular tissue, three different techniques are mainly used for the measurement of its mechanical response; simple tension, planar biaxial and inflation tests. Simple tension tests, widely used for the determination of the mechanical properties of all kinds of materials, have also been applied to soft biological tissues [see, e.g., 14, 16, 20, 42]. Among its main advantages, it is worth noting its simplicity and versatility, which allows its application to very small sized samples. Nevertheless, it allows obtaining the mechanical properties only in the testing directions. This is irrelevant when dealing with isotropic materials, but it is an important shortcoming in testing anisotropic materials such as cardiovascular tissues. A feasible possibility to complete the information provided by simple tension tests is to apply them to different tension directions [18], which partly compensates for this limitation. On the other hand, biaxial tests have been extensively used in recent years in order to obtain the mechanical properties of planar biological tissues [see, e.g., 5, 6, 27, 28, 36]. Their application allows obtaining more complete information about the mechanical response of the tissue than the simple tension test since they cause a multiaxial loading state, which is closer to the *in vivo* state. Nevertheless, their set up and preparation is much more complicated, and the interpretation of the obtained results is also difficult [34]. According to several studies [39], the small size of some biological tissues, together with the poor standardization and the influence of boundary effects, hinder the generalized use of biaxial tests. However, it is well established that biaxial tests are better than uniaxial tests if the material experiences stress in complex multiaxial configurations during its service life, and therefore the improvement of the experimental biaxial test setup for soft biological tissues is one of the fields of biomechanics in which more research effort is required. Finally, inflation tests, like biaxial tests, provide measurements of the mechanical properties of a vessel under a multiaxial loading state. Furthermore, the manipulation of the testing specimens is minimal, which notably reduces the influence of the sample preparation process on the measurements. For this reason, this testing technique has been widely used for the determination of the mechanical properties of blood vessels [see, e.g., 1, 3, 4, 13, 15, 43, 44].

The setup conditions for biaxial tests are still the subject of debate [see, e.g., 7, 8, 24, 46, 48, 50, 51]. One of the major challenges is attaching the sample to the loading system. Some studies suggest that the small size of biological tissues, the influence of boundary effects on the experimental results and the appearance of stresses and shear forces on the fixing devices have put into question the feasibility of using biaxial tests for non-linear anisotropic biological tissues [34], whereas others suggest that it is worth learning the biaxial test configuration although much remains to be done in order to better understand it [46, 49]. Despite efforts to determine an accurate method of attaching the sample edges during biaxial tests, there is still no clear understanding of the influence of the boundary effects on the results obtained during these experimental tests. Tabs or other similar extensions of the sample, such as those commonly used to create samples for uniaxial tensile tests, produce significant non-uniformities in the gauge area [48]. In addition, tabs are not practical because of the limited size of the biological tissues from which samples are cut. Although clamps or glue have been used [25, 26, 41, 50, 51], these methods produce high strains in the regions between the clamped or glued areas and lateral strain is significantly impeded. Discrete attachment points along each edge of the sample in the form of sutures [8, 22, 27, 28, 40, 48, 50, 51] have also been used. Sutures allow lateral strains and, as experiments on clamped and sutured pericardial tissue show, do not produce the artificially raised stiffnesses associated with clamps. However, point attachments produce stress concentrations and localized deformations, and the results can be affected by the number of attachment points used [7, 48]. The use of empirical correction factors to improve the measured force-stress relationship during biaxial tests has also been proposed [24]. Jacobs et al. [24] used FEM to quantify the load transmission from the clamps to the region of interest in biaxial tension and to formulate a correction factor that can be used to determine stresses in the region of interest. Additionally, computational Finite Element (FE) models can help to study the effect of these various boundary conditions on strain and stress fields within a sample [7, 33, 46, 48]. Simón-Allué et al. [46] studied the effects of boundary conditions and strain monitoring on the estimation of the constitutive parameters of elastic membranes by biaxial tests, analyzing the effects of geometry, different gripping methods and strain monitoring. They reported that the St Venant principle indicated that for medium or large samples the gripping method had no effect on the material parameters or the strain

distribution at the center of the sample. Sun et al. [48] examined the effects of boundary conditions, including varying the number of suture attachments and using different gripping methods, sample shapes, and material axis orientations. The results demonstrated strong boundary effects with the clamped methods, while the suture attachment methods demonstrated minimal boundary effects. Eilaghi et al. [7] concluded from their results that sample design and attachment significantly affected the uniformity of the strain field produced in biaxial tests. Nolan and Mcgarry [34] recently studied the problem associated with the calculation of material stress from measured force in standard biaxial tests. They concluded that localised unmeasured shear forces occur at the clamps due to stretching of the orthogonal clamp (negative shear force) and as a result of the material Poisson effect (positive shear force). These forces, which are highly dependent on the sample geometry and the clamp displacement ratio, can not be quantified and this has significant implications for the calculation of material stress from simplified force-equilibrium relationships. They also claim that commonly accepted formulae for the estimation of material stress in the central region of a cruciform sample are highly inaccurate. A reliable empirical correction factor for the general case of isotropic materials must be a function of the sample geometry and the biaxial clamp displacement ratio. Finally, they assert that a correction factor for the general case of non-linear anisotropic materials is not feasible and that inverse FE analysis should be used as a practical means of interpreting experimental data. Fehervaryn et al. [8] recently investigated varying testing and data analysis methods and their effect on the quality of the parameter fitting results on planar biaxial tests using rakes and concluded that inhomogeneities can be reduced to a minimum for wise choices of testing conditions and analysis methods, but never completely eliminated.

Within this context, the aim of the present study is to further investigate the accuracy of calculated material stress from measured force during biaxial tests. The stresses on the area free from edge effects can be computed by assessing uniformity of the stress field or by finite element modelling. The area free from edge effects depends on the gripping methods used during the test, the size and shape of the sample, among others. Further studies should be carried out to remedy this shortcoming, especially, for non-linear anisotropic materials, which according to the study of Nolan and Mcgarry [34], are not suitable for biaxial tests.This is accomplished carrying out a FE study to compare the biaxial mechanical response of two arteries with different degree of anisotropy (ascending aorta and pulmonary artery tissue samples) under two different gripping methods: (i) a system with noodle clamps and (ii) a clamped system with needles which leave the specimen's edges free to expand laterally. It is hypothesized that the physical basis for the setup of biaxial tests has not yet been well established.

2 | MATERIALS AND METHODS

2.1 | Biaxial experiments

Two biaxial experiments were considered, one for ascending thoracic porcine aorta [37] and one for pulmonary porcine artery, to test the accuracy of calculated material stress from measured force during biaxial tests. These tissues were not randomly chosen. It is well known that the behaviour of the ascending aorta could be considered quasi-isotropic from the point of view of biaxial tests (similar response for circumferential and longitudinal directions) [38]. However, the pulmonary artery has a strongly anisotropic behaviour. Thereby, two types of biological soft tissues with different degree of anisotropy are included in our study.

Tests were carried out in a high precision drive system adapted for biological specimens, the Instron BioPuls^{TM} low-force planar-biaxial testing system (load capacity of the cells:5N). Square samples (25x25 mm) were mounted in the planar-biaxial machine by connecting four carriages with noodle clamps, immersed in a bath filled with Phosphate-buffered saline (PBS) and maintained at 37ºC by a heater-circulation. Load controlled tests were performed at peak tension ratios in circumferential and longitudinal directions (P_c : P_l=60:60 kPa). For the deformation measurements during biaxial testing, several randomized markers were placed on the surface of the vessel and the lengths between the two markers in each direction were measured by a Digital Image Correlation (DIC) Strain Master LaVision System equipped with two high performance digital cameras (Imager M-lite 2M). For image post-processing in DaVis software, we used a Gaussian filter, as matching Criterion the normalized sum of square differences criteria and bi-cubic spline interpolant. For more detail about DIC parameters see table 1.

The deformation gradient **F** was also measured optically by tracking the movements of the markers. Shear strains were computed and were found to be small, and therefore were not accounted for in the constitutive model. Given negligible shear components and the incompressibility assumption, the Cauchy stresses were determined as

$$\sigma_{c,l} = \frac{F_{c,l}}{A}\lambda_{c,l}, \tag{1}$$

where $F_{c,l}$ and $\lambda_{c,l}$ are the load registered by the biaxial machine and the stretch measured by the DIC technique in circumferential (c) and longitudinal (l) directions, respectively, and A is the nominal cross-section of the sample. The nominal cross-section

DIC Hardware Parameters	
Camera	Imager M-lite 2M
Image Resolution	1600x1200
Lens	CC3516-2M Iris C-Mount Lens PENTAX 35mm F1/1.6 2/3”
Aperture	F1.6
Field-of-View	50 mm
Image Scale	28.37 pixels/mm
Stereo-Angle	31°
Stand-off Distance	316 mm
Image Acquistion Rate	10 Hz
Patterning Technique	Spray paint with black ink stamped speckles
Pattern Feature Size (approximate)	3 pixels / 0.1 mm

DIC Analysis Parameters	
DIC Software	DaVis 8.4
Image Filtering	Gaussian filter
Subset Size	15 pixels / 0.5 mm
Step Size	5 pixels / 0.16 mm
Subset Shape Function	Affine
Matching Criterion	Normalized sum of square differences (NSSD)
Interpolant	Bi-cubic spline
Strain Window	20 data points
Virtual Strain Gauge Size	125 pixels / 4.0 mm
Strain Formulation	Green-Lagrange
Post-Filtering of Strains	Spatial filter
Displacement Noise-Floor	$\pm$ 300μm

TABLE 1 DIC parameters.

($A = t_{c,l} w_{l,c}$) of the sample was obtained by two methods: measuring the distance between holes or using the whole area of the sample to take into account the quasi-zero stress outlying areas effect. $t_{c,l}$ and $w_{c,l}$ are the sample thickness and the considered width, respectively.

According to Equation 1, if the cross-section of the sample is uniform, the stresses along it should theoretically be constant (Figure 1.a), but in fact this is not the case. The cross-section of the sample is not uniform around the area of the needles, causing a peak of stresses in this area (Figure 1.b). For this reason, the distribution of stresses is commonly measured only at the central area of the samples where, if the biaxial experimental results are valid, it should be uniform. However, differences between the theoretical and real Cauchy stress along the central part of the sample could lead to significant errors in the estimation of the mechanical properties.

2.2 | Constitutive model for tissue

All the tissue samples were modelled as nonlinear, hyperelastic, and anisotropic, defined by two families of fibre materials [19]. In addition, the tissues were assumed to be incompressible [2], that is $det(\mathbf{F}) = \lambda_1 \lambda_2 \lambda_3$, where $\mathbf{F}$ represents the deformation gradient tensor and λ_i with i=1,2 and 3, the stretches in the principal directions. Given that this hyperelastic and anisotropic material is not included in the ABAQUS 6.14 library, an in-house user subroutine *UMAT* was written to define the mechanical behaviour. The behaviour of the tissue was modelled by using the strain energy function proposed by Holzapfel et al. [18],

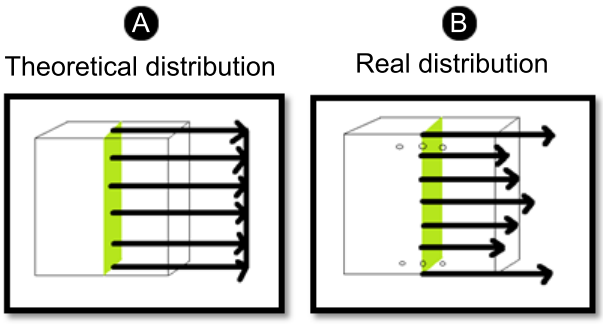

FIGURE 1 (a) Theoretical and (b) real stress distribution at the cross-section of the sample.

$$\Psi = \mu[I_1 - 3] + \\ + \frac{k_1}{2k_2}\left[\exp\left(k_2\left[\rho[I_4 - 1]^2 + [1-\rho][I_1 - 3]^2\right]\right) - 1\right] + \frac{k_3}{2k_4}\left[\exp\left(k_4\left[\rho[I_6 - 1]^2 + [1-\rho][I_1 - 3]^2\right]\right) - 1\right], \tag{2}$$

where $\mu > 0$, $k_1 > 0$ and $k_3 > 0$ are stress-like parameters and $k_2 > 0$ and $k_4 > 0$ are dimensionless parameters. The $0 \leq \rho \leq 1$ parameter is also dimensionless and accounts for the fibre dispersion. I_1 is the first invariant of the Cauchy-Green tensor characterizing the isotropic mechanical response of the elastin [12, 29], $\mathbf{C} = \mathbf{F}^T\mathbf{F}$, $I_4 = \mathbf{m}_0 \cdot \mathbf{C}\mathbf{m}_0$ and $I_6 = \mathbf{n}_0 \cdot \mathbf{C}\mathbf{n}_0$ are invariants which can be expressed as a function of the main stretches and depend on the direction of the family of fibres at a material point $\mathbf{X}$, that is defined by the unit vectors field $\mathbf{m}_0$ and $\mathbf{n}_0$ [47]. The function represents the strain energy stored in a composite material reinforced in two preferred directions represented by the invariants I_4 and I_6. Given that each family of fibres represents the main direction of collagen bundles that are orientated in a helicoidal manner, both families were assumed to have the same mechanical response ($k_3 = k_1$, $k_4 = k_2$) and the anisotropy directions were assumed to be helically oriented at $\pm\,\theta$ degrees with respect to the circumferential direction [17].

The material parameters for the constitutive law of each tissue were obtained from previously presented experimental data. The experimental results were fitted using the Levenberg-Marquardt minimization algorithm with the help of a self-made code written in MATLAB [31]. Table 2 shows the experimental stress-stretch model parameter identification fitted using the Levenberg-Marquardt minimization algorithm [31]. The normalized mean square root error (ε) which is defined as $\varepsilon = \frac{\sqrt{\frac{\chi^2}{n-q}}}{\mu}$ was used to check the goodness of the fit, where q is the number of parameters of the (SEF), n is the number of data points, $n - q$ is the number of degrees of freedom, and μ is the mean stress. Convergence to the global minimum is difficult to achieve and the final results depended strongly on the initial guess. This problem was noted earlier and reported by Fung [10] among many others. For this reason, the fits were performed multiple times starting with randomized parameters. However, the model involves a small number of material parameters, so that a least-squares procedure avoids problems of nonuniqueness associated with their sensitivity to small changes in the data [10, 19]

	$\mu[kPa]$	$k_1[kPa]$	$k_2[-]$	$\rho[-]$	$\theta[^\circ]$	$\varepsilon[-]$
Ascending Aorta	13.1	9.86	12.4	0.41	37.35	0.085
Pulmonary Artery	7.09	9.31	19.4	0.0831	29	0.073

TABLE 2 Material parameters used in the finite element analysis for both the artery aorta and pulmonary artery.

2.3 | FEM sample geometry and boundary conditions

A three-dimensional (3D) geometry corresponding to a rectangular volume with a section of 25 mm x 25 mm and a thickness of 2.1 mm was modelled in the commercial FE code ABAQUS 6.14 (Dassault Systemes, Vélizy-Villacoublay, France). Three holes were made along the outer portion of the perimeter of each attachment point, where the clamping device is fixed. It should be noted that three points is the minimum number of attached noodle suggested by Eilaghi et al. [7]. These attachment points of 0.3 mm radius are spaced 2.72 mm apart, and their centreline is 2.88 mm from the edge of the sample. In addition, the first of the three holes is located 9.78 mm from the edge (Figure 2.a). FE concretisation was performed on a mesh of 26728 linear element 8 node brick and a hybrid formulation with a typical edge length of 0.5 mm and 34095 nodes. The mesh was made as symmetric as possible in order to match the centreline of the sample and the direction of the load. In addition, the sample thickness is meshes with 4 layers of elements (Figure 2.b). The same geometry and mesh were used for all computational models.

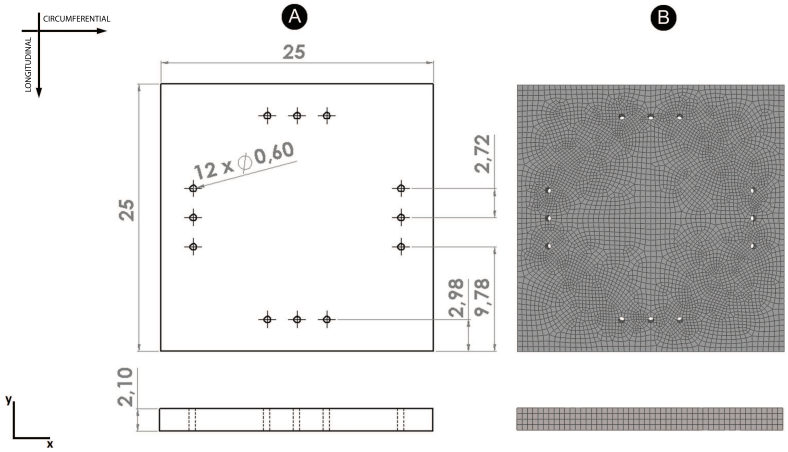

FIGURE 2 (a) Geometry and dimensions of the tissue sample model. Longitudinal and transversal sections. (B) Mesh.

Two sets of boundary conditions were studied (Figure 3). The first set is a system with needles which leave the specimen's edges free to expand laterally. The axial displacements were constrained at the contour of the holes. The longitudinal displacement was allowed, whereas the circumferential displacement was defined using the values obtained during the experimental biaxial tests around the holes. The second set consists of a system with needles, but the needles are joined to the clamps in such a way that the perpendicular movement to the pull direction is constrained but not rotation. The axial displacements were also constrained at the contour of the holes and the displacements to the direction of movement was defined using the values obtained during the experimental biaxial tests around the holes.

3 | RESULTS

Figure 4 shows the contour maps of the Cauchy stresses in the longitudinal and circumferential directions (S11 and S22) and the shear stresses (S12) for the two types of tissue (pulmonary artery and ascending aorta) for the two sets of boundary conditions. The distribution of stresses at the central area of the samples is uniform for the four studied models. In addition, the greater stresses are located at the area around the needles which are in the load direction. Therefore, if the force applied at the clamps increases, the sample will likely break around the area of the needles. Figure 4 also shows that the load applied at the clamps is not transmitted completely to the sample, since outlying areas can be found where the normal stresses are close to zero. Finally, the shear stresses are zero at the central area of the samples, confirming the hypothesis of the biaxial tests. The Cauchy stress distribution in the longitudinal and circumferential directions (S11 and S22) shows clearly that the anisotropy of the pulmonary artery is higher than the ascending aorta.

The Cauchy stresses and nominal strains along the central section of the samples in both circumferential and longitudinal directions were obtained for each FE model. In addition, the sum of the reaction forces around the holes was the force applied

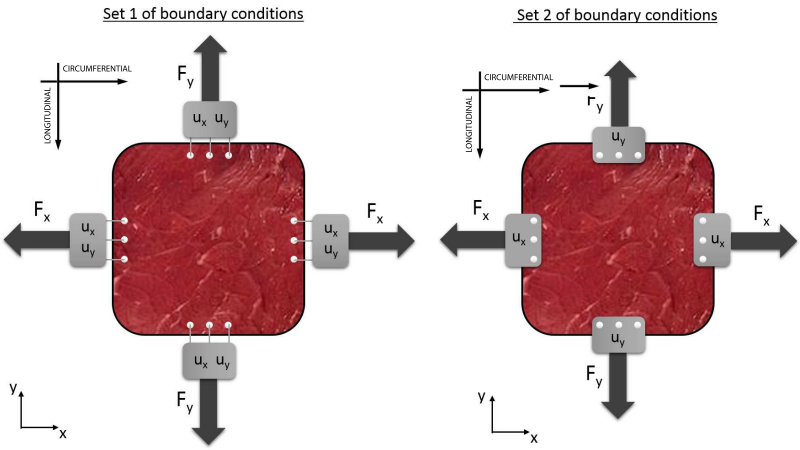

FIGURE 3 Sets of applied boundary conditions.

during the test. Therefore, using this force value, the nominal cross-section of the sample and the displacement, the theoretical value of stress at this section can be calculated following equation 1. Table 3 shows the data for the theoretical value of the stress of each sample for the Set 1 (free needles) and Set 2 (clamped needles) attachments. In all cases, the Set 2 clamped methodology showed an apparent stiffer material compared to Set 1.

TABLE 3 Data to obtain the theoretical stress at the cross-section of the sample with and without holes using Eq. 1 for Set 1 (free needles) and Set 2 (clamped needles) attachments.

			F (kN)	λ (-)	A_{whole} (mm^2)	σ_{whole} (kPa)	A_{holes} (mm^2)	σ_{holes} (kPa)
Pulmonary Artery	Set 1	Circumferential	886,45	1,074	52,5	18,13	40,404	23,81
		Longitudinal	657,26	1,115	52,5	13,96	39,984	18,33
	Set 2	Circumferential	1242,7	1,074	52,5	25,42	40,404	33,38
		Longitudinal	1094,74	1,115	52,5	23,25	39,984	30,53
Ascending Aorta	Set 1	Circumferential	967,46	1,078	52,5	19,87	40,404	26,08
		Longitudinal	802,86	1,091	52,5	16,68	39,984	21,91
	Set 2	Circumferential	1397,54	1,078	52,5	28,70	40,404	37,68
		Longitudinal	1257,17	1,091	52,5	26,13	39,984	34,30

Figure 5 compares the real circumferential and longitudinal Cauchy stresses along the sample computed by the FE model for the two types of tissue and for the two different boundary conditions. It shows the values obtained by means of the FE analysis (in blue) and the theoretical value considering both the whole sample (in green) and the sample between the holes (in red). The results show that the second set of boundary conditions underestimates the theoretical values for both the pulmonary artery and the ascending aorta and for both circumferential and longitudinal directions. The first set of boundary conditions, which leave the specimen's edges free to expand laterally, provides stress values closer to the theoretical values. In addition, for the first set of boundary conditions, the ascending aorta results are more accurate than those obtained for the pulmonary artery due to the strongly anisotropic behaviour of the latter. For the circumferential direction, the stresses are overestimated.

The errors between the stresses provided by the FE model and the theoretical stresses (both considering the whole cross-section and the cross-section with holes) are presented in Table 4 for the Set 1 (free needles) and Set 2 (clamped needles) attachments. These errors were calculated at the central point of the sample as

$$error = \frac{\sigma_{theoretical} - \sigma_{FEM}}{\sigma_{FEM}} x100. \quad (3)$$

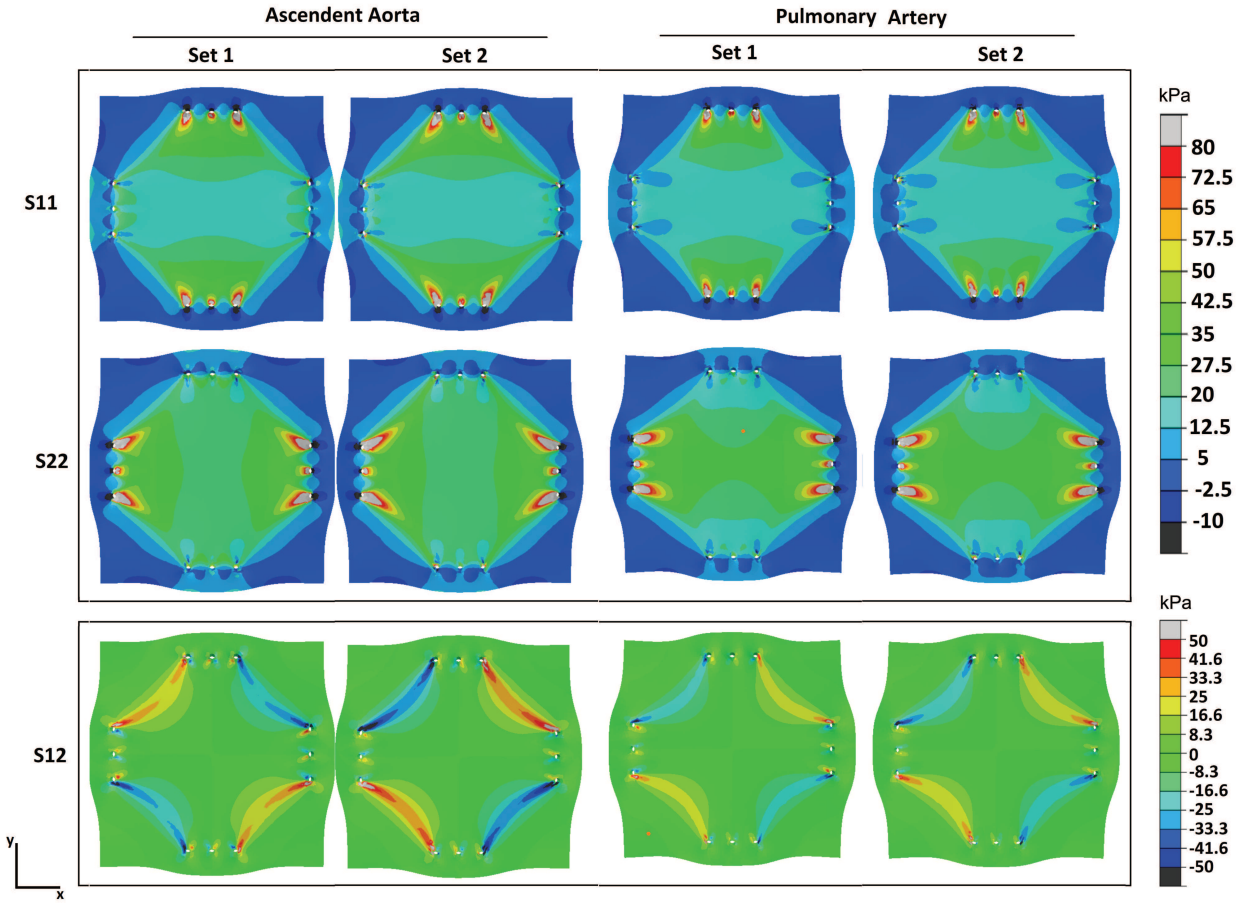

FIGURE 4 Contour maps of the normal stresses in the longitudinal and circumferential directions (S11 and S22) and the shear stresses (S12) for the two types of tissue (pulmonary artery and ascending aorta) and for the two sets of boundary conditions.

In general, Set 1 showed smaller errors than Set 2 and using a nominal area between holes proved to be more accurate than using a nominal sample area. There are no conclusions with respect to the degree of anisotropy of the material as the results showed similar errors for the pulmonary and ascending arteries. Minimal errors were found for the aorta samples in the longitudinal direction results (3%) and the maximum error in the circumferential direction for the pulmonary artery, both for Set 1.

Finally, an analysis of the stress-stretch curves computed using the real Cauchy stress and the theoretical stress computed by Equation 1 for the Set 1 (free needles) and Set 2 (clamped needles) attachments is shown in Figure 6. An analysis of this figure is crucial given that the stress-stretch curve is the aim of the experimental test in order to understand the mechanical response of the arteries and to compute a constitute parameters by fitting a SEF. Figure 6 shows that differences between the curves computed using Set 1 and Set 2 are minimal. However, the Average Reaction Force (ARF) method(Equation 1) shows lower stress values compared to the Finite Element (FE) stress methodology for highly anisotropic material like pulmonary artery. These differences are critical for the longitudinal direction. This means that the computed curves obtained by experimental show a more compliances material than the real one and the subsequent computational simulations produce lower forces or higher displacements. The differences are minimal for the ascending aorta whose mechanical response is quasi-isotropic.

4 | DISCUSSION

In this study, we have investigated the accuracy of calculated material stress from measured force during biaxial tests depending on two different gripping methods. The physical basis for the setup of biaxial tests has not yet been well established. Further studies should be carried out to remedy this situation, especially for non-linear anisotropic materials which, according to the

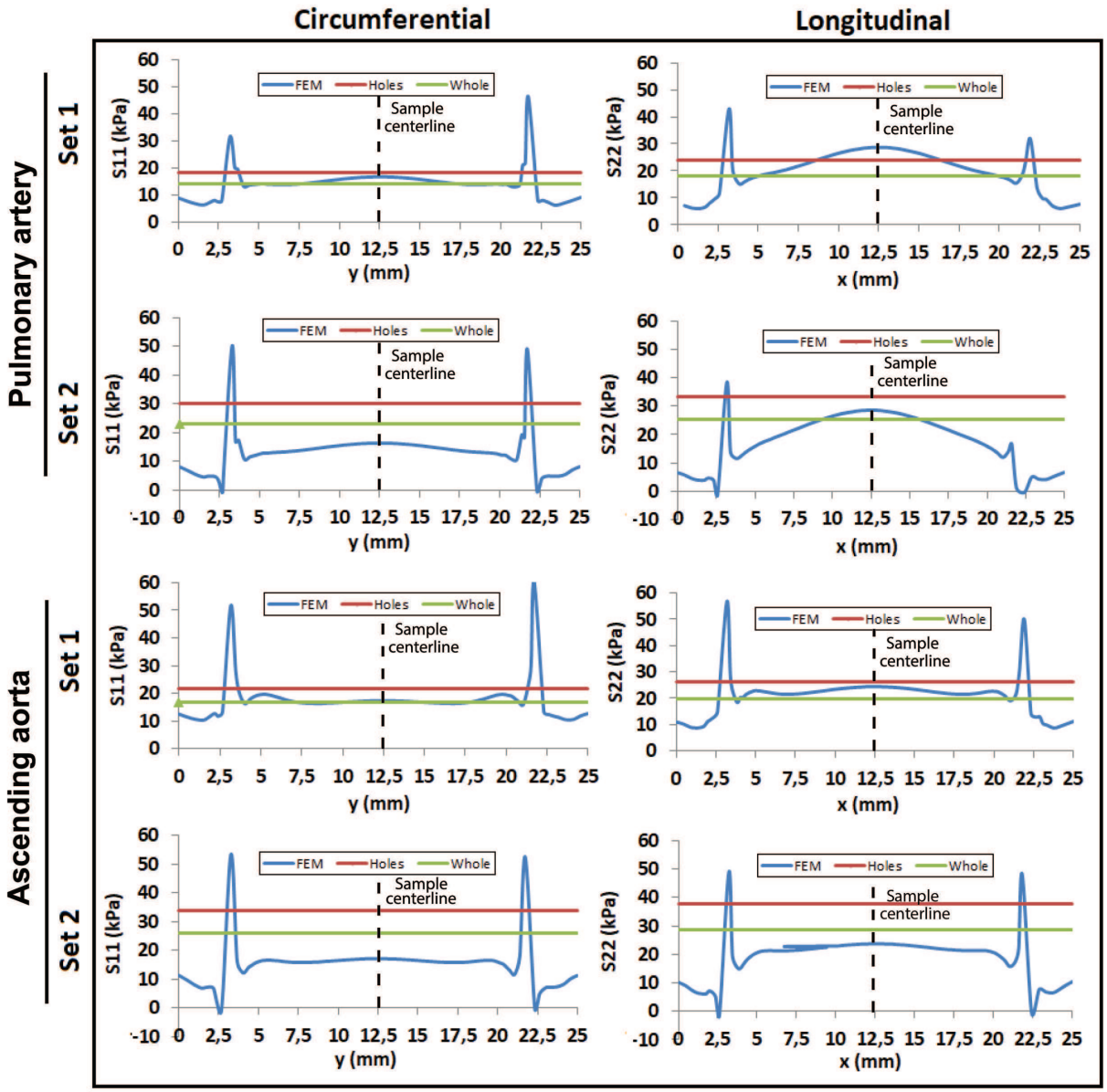

FIGURE 5 Stresses along the central cross-section or the two types of tissue (pulmonary artery and ascending aorta) and for the two sets of boundary conditions. It shows the values obtained by means of the FE analysis (in blue) and the theoretical value considering both the whole sample (in green) and the sample between the holes (in red).

study of Nolan and Mcgarry [34], are not suitable for biaxial tests. They demonstrate that commonly accepted formulae for the estimation of material stress in the central region of a cruciform specimen are highly inaccurate. A reliable empirical correction factor for the general case of isotropic materials must be a function of specimen geometry and the biaxial clamp displacement ratio. In addition, they demonstrate that a correction factor for the general case of non-linear anisotropic materials is not feasible and they suggest the use of inverse finite element analysis as a practical means of interpreting experimental data for such complex materials. Many efforts have been made in order to analyse the setup conditions of biaxial mechanical tests and definitely identify an accurate method of attaching the sample edges during these experimental tests [see, e.g., 7, 8, 24, 46, 48, 50, 51]. However, there is still no clear understanding of the influence of the boundary effects on the results obtained during these experimental tests. For that purpose, in the present study, Finite Element(FE) analyses have been combined with experimental biaxial tests. Specifically, the biaxial mechanical response of ascending aorta and pulmonary artery tissue samples has been

TABLE 4 Computed errors between the stresses provided by the FE model and the obtained theoretical stresses (both considering the whole cross-section and the cross-section with holes) for Set 1 (free needles) and Set 2 (clamped needles) attachments using Equation 3.

			Error (whole) (%)	Error (with holes) (%)
Pulmonary Artery	Set 1	Circumferential	55.9	20.1
		Longitudinal	18.8	9.4
	Set 2	Circumferential	12.1	14.6
		Longitudinal	29.5	46.3
Ascending Aorta	Set 1	Circumferential	23.3	6
		Longitudinal	3	21.5
	Set 2	Circumferential	17	36.8
		Longitudinal	34.9	50.4

examined under two different gripping methods: (i) a system with noodle clamps and (ii) a clamped system with needles which leave the specimen's edges free to expand laterally. The results of each method have been compared. We compare the theoretical stress at the cross-section of the sample using Eq. 1 with the real stress obtained by FE analysis.

Our results show that the clamped method whose joints allow the specimen's edges free to expand laterally produces stresses closer to the universally accepted formulation of biaxial material stress in the central region. However, the system with noodle clamps or rakes [8], commonly used to grip the sample, produces an alteration of the measurement stresses. This is mainly because this kind of gripping method does not allow displacement in the perpendicular direction (Figures 4 and 5). It should be noted that Eilaghi et al. [7] considered that three points represents the minimum number of attached noodles. Without loss of generality, the most adverse case has been considered for this study, so increasing the number of noodles would reduce the error on the experimental data.

According to the study of Nolan and Mcgarry [34], biaxial tests are not suitable for non-linear anisotropic materials. However, our study reveals that the clamping method used during the biaxial test is more influential and crucial than the degree of anisotropy of the material as Table 4 shows. The FE analyses were performed with two types of biological soft tissues with different degree of anisotropy. It is well known that the behaviour of the ascending aorta could be considered quasi-isotropic from the point of view of biaxial tests (similar response in circumferential and longitudinal directions). However, the pulmonary artery has a strongly anisotropic behaviour. It should be noted that neither our simulations nor the analysis of Nolan and Mcgarry [34] result in an accurate estimate of the stress at the centre of the sample. In some cases the stresses are overestimated, and in others underestimated. However, the errors in our study are lower than those found by Nolan and Mcgarry [34] since the clamping methods are different. Whereas Nolan and Mcgarry [34] used conventional clamps which do not allow movement in the perpendicular direction, we used a clamped system with needles which leave the specimen's edges free to expand laterally. While clamping the sample provides a simpler method, clamping can lead to very high stress concentrations at the clamped site and reduces the area where the material stresses are uniform. In that case, a combined experimental-numerical approach should be used, wherein the displacement on the sample surface are measured by DIC technique while material stresses are computed via FEM and inverse methodology are used to estimated the material properties [30].

The presented results should be approached with regard to their limitations. First, all the numerical analyses assumed homogeneous and incompressible materials while soft tissues are in fact more or less heterogeneous which may affect primarily the results for large samples which are naturally more heterogeneous. However, these assumptions have been widely accepted as allowable for the assessment of the biomechanical properties of cardiovascular tissues. Second, perfectly symmetric and accurate positions of clamps and needles were assumed in all the analyses. Naturally, the accuracy of the positioning of clamps or needles represents another important dependent factor influencing the stress distribution [7]. Third, it is noted that these results are not directly applicable to sutures for which higher local stress concentrations and earlier ruptures may occur because of their smaller diameter, very low bending stiffness and consequently high and varying curvature. Fourth, The biaxial stress hypothesis on the central part of the sample were verified for the experimental part using DIC and enforced by symmetry conditions on the FE model. This is the reason why we use the stress of the central node to compute FES. Watching Figures 4 and 5, the region of approximately uniform biaxial stresses is located on the central part of the samples and is more than the 30% of the sample with

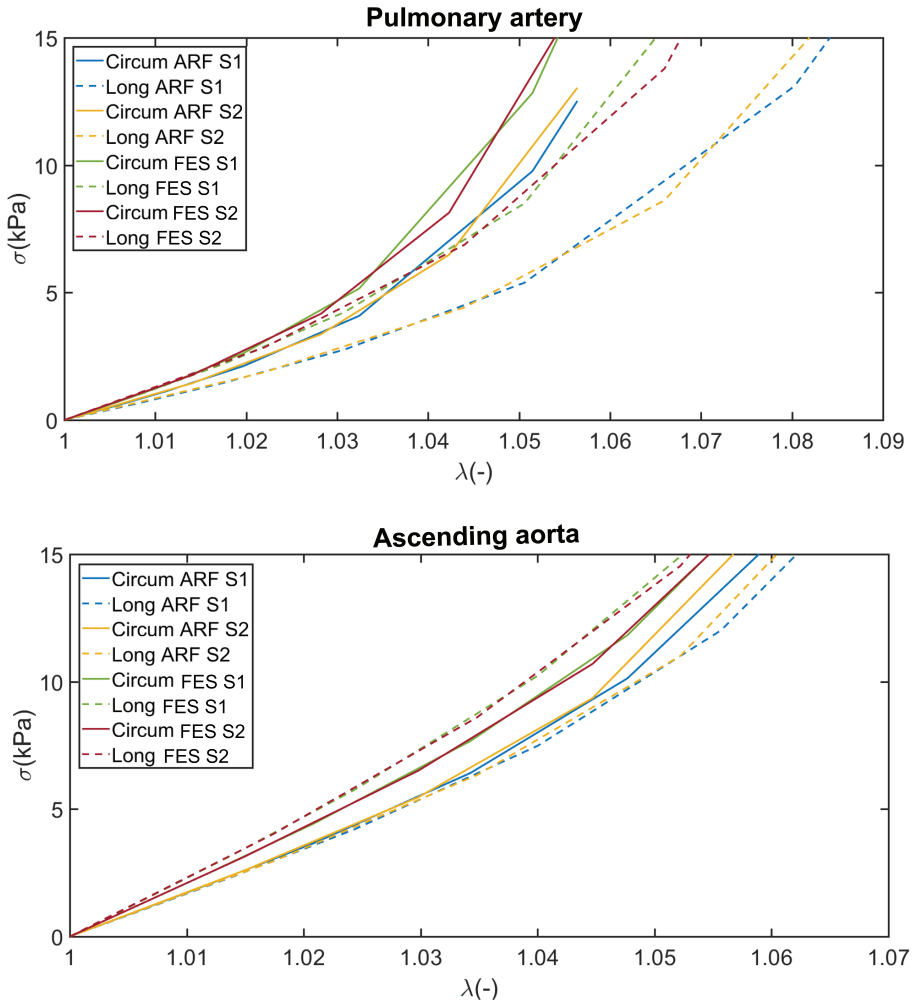

FIGURE 6 Stress-stretch curves computed using the real Cauchy stress and the theoretical stress computed by Equation 1 for Set 1 (free needles) and Set 2 (clamped needles) attachments. FES means Finite Element Stress and ARF means Average Reaction Force.

the exception of the longitudinal direction of the pulmonary artery which the area is reduced to 15%. Finally, the experiments were performed with an assumption of having the principal material directions aligned with the edges of the sample.

Despite these limitations, we can conclude that the clamped system with needles which leave the specimen's edges free to expand laterally can be used as an efficient alternative to other commonly used gripping methods for biological tissues with different degree of anisotropy.

Acknowledgments

The authors gratefully acknowledge research support from the Spanish Ministry of Science and Technology through research project DPI2016-76630-C2-1-R, the regional Government of Aragón support for the funding of the research group T24-17R: Applied Mechanics and Biomechanics (AMB), CIBER initiative and by the use of Servicio General de Apoyo a la Investigación-SAI, Universidad de Zaragoza..CIBER-BBN is an initiative funded by the VI National R&D&i Plan 2008-2011, Iniciativa Ingenio 2010, Consolider Program, CIBER Actions and financed by the Instituto de Salud Carlos III with assistance from the European Regional Development Fund. Part of the work was performed by the ICTS "NANBIOSIS" specifically by the

Tissue & Scaffold Characterization Unit (U13) and High Performance Computing Unit (U27), of the CIBER in Bioengineering, Biomaterials & Nanomedicne (CIBER-BBN at the University of Zaragoza).

Author contributions

J.A.P., M.C. and E.P. contributed to idea generation and completion of this work. A.V.C. and E.P. performed the experiments. A.V.C and J.A.P. and M.C. analysed the data. All the authors contributed to writing and reviewing the manuscript.

Financial disclosure

No financial support from other organizations unless the cited in the acknowledgements section, nor personal relationships, nor people, nor organisms biased the development of this research work.

Conflict of interest

The authors declare no potential conflict of interests.

References

[1] Carboni, M., G. W. Desch, and H. W. Weizsacker, 2007: Passive mechanical properties of porcine left circumflex artery and its mathematical description. *Medical Engineering & Physics*, **29**, no. 1, 8–16.

[2] Carew, T. E., R. N. Vaishnav, and D. J. Patel, 1968: Compressibility of the arterial wall. *Circulation Research*, **23**, 61–86.

[3] Carmines, D. V., J. H. McElhaney, and R. Stack, 1991: A piece-wise nonlinear elastic stress expression of human and pig coronary-arteries tested *in vitro*. *Journal of Biomechanics*, **24(10)**, 899–906.

[4] Cilla, M., M. Pérez, E. Peña, and M. A. Martínez, 2016: Effect of diet and age on arterial stiffening due to atherosclerosis in apoe-/- mice. annals of biomedical engineering. *Annals of Biomedical Engineering*, **44**, no. 7, 2202–2217.

[5] Cox, M. A. J., N. J. B. Driessen, R. A. Boerboom, C. V. C. Bouten, and F. P. T. Baaijens, 2008: Mechanical characterization of anisotropic planar biological soft tissues using finite indentation: Experimental feasibility. *Journal of Biomechanics*, **41**, no. 2, 422–429.

[6] Cox, M. A. J., N. J. B. Driessen, C. V. C. Bouten, and F. P. T. Baaijens, 2006: Mechanical characterization of anisotropic planar biological soft tissues using large indentation: A computational feasibility study. *ASME Journal of Biomechanical Engineering*, **128**, no. 3, 428–436.

[7] Eilaghi, A., J. Flanagan, G. Brodland, and C. Ethier, 2009: Strain uniformity in biaxial specimens is highly sensitive to attachment details. *ASME Journal of Biomechanical Engineering*, **131**, no. 091003, 1–7.

[8] Fehervaryn, H., M. Smoljkic, J. V. Sloten, and N. Famaey, 2016: Planar biaxial testing of soft biological tissue using rakes: A critical analysis of protocol and fitting process. *J Mech Behav Biomed*, **61**, 135–151.

[9] Fung, Y. C., 1990: *Biomechanics. Mechanical properties of living tissues*. Springer-Verlag.

[10] — 1993: *Biomechanics. Mechanical properties of living tissues*. Secondnd ed., Springer-Verlag, New York.

[11] Fung, Y. C., K. Fronek, and P. Patitucci, 1979: Pseudoelasticity of arteries and the choice of its mathematical expression. *American Journal of Physiology*, **237**, 620–631.

[12] Gundiah, N., M. Ratcliffe, and L. A. Pruitt, 2009: The biomechanics of arterial elastin. *Journal of the Mechanical Behavior of Biomedical Materials*, **2**, 288–296.

[13] Hayashi, K., H. Handa, S. Nagasawa, A. Okumura, and K. Moritake, 1980: Stiffness and elastic behavior of human intracranial and extracranial arteries. *Journal of Biomechanics*, **13**, no. 2, 175–179.

[14] Hayashi, K. and Y. Imai, 1997: Tensile property of atheromatous plaque and an analysis of stress in atherosclerotic wall. *Journal of Biomechanics*, **30**, 573–579.

[15] Hayashi, K., K. Mori, and H. Miyazaki, 2003: Biomechanical response of femoral vein to chronic elevation of blood pressure in rabbits. *American Journal of Physiology - Heart and Circulatory Physiology*, **284**, no. 2, 511–518.

[16] Hayashi, K., T. Washizu, N. Tsushima, R. J. Kiraly, and Y. Nose, 1981: Mechanical properties of aortas and pulmonary arteries of calves implanted with cardiac prostheses. *Journal of Biomechanics*, **14(3)**, 173–182.

[17] Holzapfel, G. A., 2000: *Nonlinear Solid Mechanics: A Continuum Approach for Engineering.*. John Wiley & Sons.

[18] Holzapfel, G. A., C. T. Gasser, G. Sommer, and P. Regitnig, 2005b: Determination of the layer-specific mechanical properties of human coronary arteries with non-atherosclerotic intimal thickening, and related constitutive modelling. *American Journal of Physiology - Heart and Circulatory Physiology*, **289**, 2048–2058.

[19] Holzapfel, G. A., T. C. Gasser, and R. W. Ogden, 2000: A new constitutive framework for arterial wall mechanics and a comparative study of material models. *Journal of Elasticity*, **61**, 1–48.

[20] Holzapfel, G. A., M. Stadler, and C. T. Gasser, 2005a: Changes in the mechanical environment of stenotic arteries during interaction with stents: Computational assessment of parametric stent designs. *ASME Journal of Biomechanical Engineering*, **127**, 166–180.

[21] Hrapko, M., J. A. Van Dommelen, G. W. Peters, and J. S. Wismans, 2008: The influence of test conditions on characterization of the mechanical properties of brain tissue. *ASME Journal of Biomechanical Engineering*, **130**, no. 3, 031003.

[22] Humphrey, J., R. Strumpf, and F. C. P. Yin, 1990: Biaxial mechanical behavior of excised ventricular epicardium. *American Journal of Physiology*, **259**, H101–H108.

[23] Humphrey, J. D., 2001: Stress, strain, and mechanotransduction in cells. *ASME Journal of Biomechanical Engineering*, **123**, no. 6, 638–641.

[24] Jacobs, N., D. Cortes, E. Vresilovic, and D. Elliott, 2013: Biaxial tension of fibrous tissue: using finite element methods to address experimental challenges arising from boundary conditions and anisotropy. *Journal of Biomechanical Engineering*, **135**, no. 2, 021004.

[25] Kanyanta, V. and A. Ivankovic, 2010: Mechanical characterisation of polyurethane elastomer for biomedical applications. *Journal of the Mechanical Behavior of Biomedical Materials*, **3**, 51–62.

[26] Langdon, S. E., R. Chernecky, C. A. Pereira, D. Abdulla, and J. M. Lee, 1999: Biaxial mechanical structural effects of equibiaxial strain during crosslinking of bovine pericardial xenograft materials. *Biomaterials*, **20**, no. 2, 137–153.

[27] Lanir, Y. and Y. C. Fung, 1974: Two-dimensional mechanical properties of rabbit skin-I. Experimental system. *Journal of Biomechanics*, **7**, no. 1, 29–34.

[28] — 1974: Two-dimensional mechanical properties of rabbit skin-II. Experimental results. *Journal of Biomechanics*, **7**, no. 2, 171–174.

[29] Lillie, M., R. Shadwick, and G. J.M., 2010: Mechanical anisotropy of inflated elastic tissue from the pig aorta. *Journal of Biomechanics*, **43**, 2070–2078.

[30] Macrae, R. A., K. Miller, and B. J. Doyle, 2016: Methods in Mechanical Testing of Arterial Tissue: A Review. *Strain*, **52**, 380–399.

[31] Marquardt, D. W., 1963: An algorithm for least-squares estimation of nonlinear parameters. *SIAM Journal on Applied Mathematics*, **11**, 431–441.

[32] Miller, K., 2001: How to test very soft biological tissues in extension? *Journal of Biomechanics*, **34**, no. 5, 651–657.

[33] Nielsen, P. M. F., P. J. Hunter, and B. H. Smaill, 1991: Biaxial testing of membrane biomaterials: Testing equipment and procedures. *ASME Journal of Biomechanical Engineering*, **113**, no. 3, 295–300.

[34] Nolan, D. and J. Mcgarry, 2016: On the correct interpretation of measured force and calculation of material stress in biaxial tests. *Journal of the Mechanical Behavior of Biomedical Materials*, **53**, 187–199.

[35] Oyen, M. L., 2011: *Handbook of nanoindentation with biological applications*. Pan Stanford Publishing Pte. Ltd. Singapore.

[36] Pandit, A., X. Lu, C. Wang, and G. S. Kassab, 2005: Biaxial elastic material properties of porcine coronary media and adventitia. *American Journal of Physiology - Heart*, **288**, H2581–H2587.

[37] Peña, J., M. Martínez, and E. Peña, 2015: Layer-specific residual deformations and uniaxial and biaxial mechanical properties of thoracic porcine aorta. *Journal of the mechanical behavior of biomedical materials*, **50**, no. 1, 55–69.

[38] Peña, J. A., V. Corral, M. A. Martínez, and E. Peña, 2018: Over length quantification of the multiaxial mechanical properties of the ascending, descending and abdominal aorta using Digital Image Correlation. *J Mech Behav Biomed*, **77**, 434–445.

[39] Sacks, M., 2000: Biaxial mechanical evaluation of planar biological materials. *Journal of Elasticity*, **61**, 199–246.

[40] Sacks, M. S. and W. Sun, 2003: Multiaxial mechanical behavior of biological materials. *Annual Review of Biomedical Engineering*, **5**, 251–284.

[41] Sakuma, I., Y. Nishimura, C. K. Chui, E. Kobayashi, H. Inada, X. Chen, and T. Hisada, 2003: *In vitro Measurement of Mechanical Properties of Liver Tissue under Compression and Elongation Using a New Test Piece Holding Method with Surgical Glue*, Springer Berlin Heidelberg, Berlin, Heidelberg. 284–292.

[42] Schulze-Bauer, C. A. J., C. Mörth, and G. A. Holzapfel, 2003: Passive biaxial mechanical response of agel human iliac arteries. *ASME Journal of Biomechanical Engineering*, **125**, 395–406.

[43] Schulze-Bauer, C. A. J., P. Regitnig, and G. A. Holzapfel, 2002: Mechanics of the human femoral adventitia including the high-pressure response. *American Journal of Physiology - Heart and Circulatory Physiology*, **282**, no. 6, 2427–2440.

[44] Sáez, P., A. García, E. Peña, T. C. Gasser, and M. A. Martínez, 2016: Microstructural quantification of collagen fiber orientations and its integration in constitutive modeling of the porcine carotid artery. *Acta Biomaterialia*, **33**, 183–193.

[45] Silver, F. H., P. B. Snowhill, and D. J. Foran, 2003: Mechanical behavior of vessel wall: A comparative study of aorta, vena cava, and carotid artery. *Annals of Biomedical Engineering*, **31**, 793–803.

[46] Simón-Allué, R., A. Cordero, and Peña, 2014: Unraveling the effect of boundary conditions and strain monitoringon estimation of the constitutive parameters of elastic membranesby biaxial tests. *Mechanics Research Communications*, **57**, 82–89.

[47] Spencer, A. J. M., 1971: Theory of invariants. *Continuum physics. Academic Press, New York*, 239–253.

[48] Sun, W., M. S. Sacks, and M. J. Scott, 2005: Effects of boundary conditions on the estimation of the planar biaxial mechanical properties of soft tissues. *ASME Journal of Biomechanical Engineering*, **127**, no. 4, 709–715.

[49] Waldman, S. and J. Lee, 2005: Effect of sample geometry on the apparent biaxial mechanical behaviour of planar connective tissues. *Biomaterials*, **26**, no. 35, 7504–7513.

[50] Waldman, S. and M. Lee, 2002: Boundary conditions during biaxial testing of planar connective tissues. part 1: dynamic behavior. *Journal of Materials Science: Materials in Medicine*, **288**, no. 6, H2581–7.

[51] — 2002: Boundary conditions during biaxial testing of planarconnective tissues. part 2: fiber orientation. *Journal of Materials Science: Materials in Medicine*, **21**, 1215–1221.

[52] World Health Organizat, 2017: *World health statistics 2017: monitoring health for the SDGs, Sustainable Development Goals*.

How to cite this article: Cilla M., A. V. Corral, J.A. Peña, and E. Peña (2019), Analysis of the biaxial stress hypothesis for arteries by Finite Element Analysis, *Strain*, *2019;00:1–6*.